

Heat capacity and relaxation dynamics of glassy films: A lattice model study

Qiang Zhai ¹, Xin-Yuan Gao ², Hai-Yao Deng ³, Chun-Shing Lee,⁴ Sen Yang,¹ Ke Yan,^{5,*} and Chi-Hang Lam ^{6,†}

¹*MOE Key Laboratory for Nonequilibrium Synthesis and Modulation of Condensed Matter, School of Physics, Xi'an Jiaotong University, Xi'an, Shaanxi 710049, China*

²*Department of Physics, The Chinese University of Hong Kong, Shatin, New Territories, Hong Kong, China*

³*School of Physics and Astronomy, Cardiff University, 5 The Parade, Cardiff CF24 3AA, Wales, United Kingdom*

⁴*School of Science, Harbin Institute of Technology (Shenzhen), Shenzhen 518055, China*

⁵*School of Mechanical Engineering, Xi'an Jiaotong University, Xi'an, Shaanxi 710049, China*

⁶*Department of Applied Physics, Hong Kong Polytechnic University, Hong Kong, China*



(Received 9 September 2024; accepted 9 December 2024; published 6 January 2025)

We study the calorimetric properties and structural relaxation of glassy films using a distinguishable particle lattice model (DPLM). We determine the glass transition temperature versus film thickness from the heat capacity during heating as well as from the local relaxation time. The results based on both approaches are in good agreement with the experimentally observed Keddie-Cory-Jones relation. The thus demonstrated interplay between calorimetric properties and structural relaxation is further corroborated by successfully reconstructing the simulated heat capacity during heat and cooling from the local relaxation times. Our results suggest DPLM as a useful lattice model for studying glassy films.

DOI: [10.1103/PhysRevE.111.015406](https://doi.org/10.1103/PhysRevE.111.015406)

I. INTRODUCTION

Glass transition remains puzzling despite intensive and extensive studies [1–5]. Interesting phenomena have been discovered over the past few decades in the study of confined systems such as glassy films [6–17]. Spatial confinement was found to bear a significant impact on the vitrification process of liquid films. For example, the glass transition temperature, one of the main characteristics of glass transition, was measured lower for thinner polystyrene films [6]. The transition temperature for a film of thickness h , denoted by $T_{g,h}$, empirically follows the Keddie-Cory-Jones relation,

$$\frac{T_{g,h}}{T_{g,\infty}} = 1 - \left(\frac{A}{h}\right)^\delta, \quad (1)$$

where $T_{g,\infty}$ is the transition temperature of a bulk material while A and δ are fitting parameters. It has been suggested that there is a decoupling between molecular mobility and reduction of transition temperature for glasses upon confinement [18]. Questions as regards the physical mechanism underlying the reduction of transition temperature are yet to be answered [15,16].

In addition, spatially resolved measurements reveal that films do not vitrify uniformly. The regions deeper into the bulk vitrify at a much higher temperature than those near the free surface. The local transition temperature at depth z (measured from the free surface), denoted by $T_g(z)$, displays a gradient that can span hundreds of nanometers [19]. Simulations [20] show that the overall transition temperature $T_{g,h}$ for a film is

not an arithmetic average over the local transition temperature $T_g(z)$. The exact relation between $T_g(z)$ and $T_{g,h}$ remains to be clarified [20,21].

In the present work, we employ a distinguishable particle lattice model (DPLM) to study the glassy properties of films. The DPLM captures the random energy landscape of glassy systems via particle distinguishability. It has successfully reproduced a wide set of experimentally observed glassy phenomena, including the Kovacs paradox [22] and effect [23], broad distribution of thermodynamic and kinetic fragilities [24], large heat capacity overshoot for fragile glasses [25], two-level systems [26], dynamical facilitation as seen in diffusion coefficient power laws [27], Kauzmann's paradox [28] and, more recently, the existence of a surface mobile layer [29].

The purpose here is multifold. In the first place, we reproduce the Keddie-Cory-Jones relation, Eq. (1), for DPLM films. We determine $T_{g,h}$ by studying the energy relaxation of our films through calorimetric measurements, which are in general analogous to thermal expansivity measurements in experiments. The specific heat capacity, $C_h(T)$, was computed and an overshoot during heating was observed, which was then used to determine $T_{g,h}$ following the common protocol [25,30]. The as-obtained $T_{g,h}$ is well described by Eq. (1) with $A \approx 1.31$ and $\delta \approx 1.35$, and also matches experimental results on polystyrene (PS) films.

Further, we analyze the depth-resolved relaxation dynamics of DPLM films and show that the depth-resolved α -relaxation time, denoted by $\tau_\alpha(z)$ at depth z , can be used to estimate the heat capacity of the films. Specifically, we first use $\tau_\alpha(z)$ to determine the local transition temperature $T_g(z)$. We then show that, aided by the functional form of the heat capacity for bulk materials, written as $C_\infty(T/T_{g,\infty})$, the

*Contact author: yanke@mail.xjtu.edu.cn

†Contact author: C.H.Lam@polyu.edu.hk

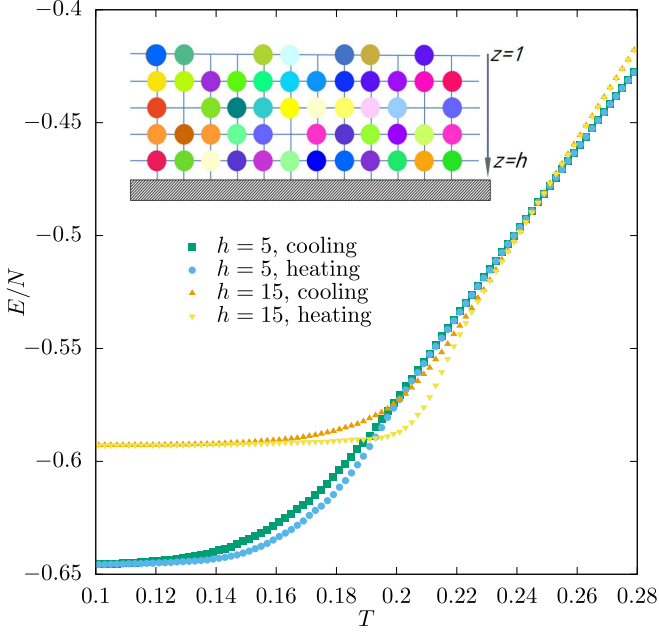


FIG. 1. Energy evolution of representative samples during a heating and cooling cycle. Inset: Schematic of the film lattice.

heat capacity for a film can be approximated as the arithmetic average of the heat capacities for its constituting layers, each evaluated using $C_\infty[T/T_g(z)]$, namely,

$$C_h(T) \approx \frac{1}{h} \int_0^h dz C_\infty\left(\frac{T}{T_g(z)}\right), \quad (2)$$

which agrees reasonably well with the direct simulations.

Finally, we have evaluated $T_{g,h}$ from the overall α -relaxation time for a film $\tau_{\alpha,h}$. The resulting $T_{g,h}$ again follows Eq. (1) but with slightly different values of A and δ . These results demonstrate a close interplay between nonequilibrium thermal properties and the relaxation of glassy films.

The rest of the paper is organized as follows. We first briefly introduce the model in Sec. II. Then we report the calorimetric measurements in Sec. III A, followed by the relaxation dynamics in Sec. III B. In Sec. III C we show that $C_h(T)$ can be related to $C_\infty(T)$ via $\tau_\alpha(z)$.

II. DPLM FILM

The DPLM film studied here has already been described in Ref. [29]. It consists of N distinguishable particles, each of its own type, living on a square lattice with thickness h and length L (inset of Fig. 1). A lattice site is either empty or singly occupied by a particle. The absence of a particle is called a void. The periodic boundary condition is applied along the direction of L and the open boundary condition along the direction of z . The film confined to $1 \leq z \leq h$ is supported on a substrate on one termination (designated $z = h$) and has a free surface on the other termination ($z = 1$). The energy of the film is given by

$$E = \sum_{\langle i,j \rangle} V_{s_i s_j} n_i n_j + \epsilon_{\text{top}} \sum_{i:z_i=1} n_i + \epsilon_{\text{bot}} \sum_{i:z_i=h} n_i. \quad (3)$$

Here s_i labels the type of the particle at site i , $V_{s_i s_j}$ gives the interaction energy between the particle at site i and the particle at an adjacent site j , n_i is the particle occupation at site i so that $n_i = 1$ if site i is occupied by a particle or $n_i = 0$ if the site is occupied by a void, and z_i is the z coordinate (i.e., depth) of site i . The last two sums in Eq. (3) are included to account for the interfacial excess energy. Throughout the paper we use $\epsilon_{\text{top}} = 1.124$ and $\epsilon_{\text{bot}} = -0.5$ for the particles at the vacuum and substrate interfaces, respectively. The interaction energy $V_{s_i s_j}$ is sampled from the *a priori* distribution,

$$g(V) = G_0/(V_1 - V_0) + (1 - G_0)\delta(V - V_1), \quad (4)$$

where $V_0 = -0.5$, $V_1 = 0.5$, and $G_0 = 0.7$ are parameters chosen for the study. As shown previously [24], these parameters correspond to a moderately strong glass.

The dynamics of the particles are purely dissipative after the Metropolis algorithm. A particle can hop to an adjacent empty site with the acceptance rate

$$w = w_0 \exp[-\Delta E \Theta(\Delta E)/k_B T], \quad (5)$$

where ΔE is the energy change due to the hop, $\Theta(x) = 1$ if $x > 0$ or $\Theta(x) = 0$ otherwise, $w_0 = 10^6$ is the attempt frequency, and k_B is the Boltzmann constant. We work with units $k_B = 1$ throughout. Detailed balance is guaranteed by the algorithm.

III. RESULTS AND DISCUSSIONS

A. Calorimetric measurements

The calorimetric measurements are performed according to standard heat bath protocols. A sample is first prepared in thermodynamic equilibrium at a bath temperature of $T = 0.28$. It is then cooled down from $T = 0.28$ at the rate $Q_c = 10^{-4}$. Once reaching $T = 0.10$, the sample is heated back at the same rate. Figure 1 displays the energy per particle E/N against T for two representative films with $h = 5$ and $h = 15$, respectively. A hysteresis is observed between the heating and cooling process due to the falling out of thermodynamic equilibrium, similar to observations on bulk samples [25,31]. The hysteresis is less pronounced for the thinner film, indicating a lower glass transition temperature $T_{g,h}$.

The heat capacity per particle of the film is calculated as $C_h = \frac{1}{N} dE/dT$. The results are shown in Fig. 2. The heat capacity by the heating process, for films regardless of their thicknesses, shows a main overshoot, in agreement with experimental measurements [31] and previous bulk DPLM simulations [25]. Besides that, the peak of the overshoot shifts towards lower temperatures for thinner films. The magnitude of C_h on the higher-temperature side of the peak also decreases with decreasing film thicknesses. Note that the peak from the $h = 5$ film shifts to a much lower T . This is because the whole film now admits drastic surface enhanced dynamics, as will be further illustrated by depth-resolved measurements below. Those observations are consistent with differential-scanning-calorimetry (DSC) measurements on nanospheres [32] and thin films [33].

The glass transition temperature $T_{g,h}$ is determined from the heating curve $C_h(T)$ using the method described in Ref. [30]; see inset in Fig. 3. In Fig. 3, the as-determined $T_{g,h}$ is exhibited

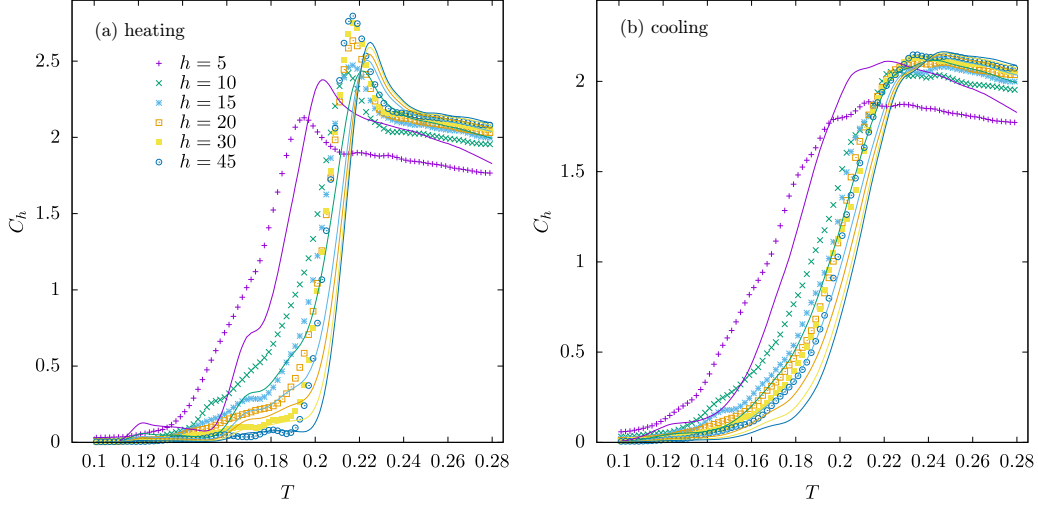


FIG. 2. Symbols: Specific heat capacity C_h from (a) heating and (b) cooling simulations at rate $Q_c = 10^{-4}$. Lines: Theoretically estimated specific heat capacity of films as an average over the contributions from individual layers using Eq. (2) and the local relaxation time.

against film thickness h after rescaling by a lattice constant $a_0 = 0.81$ nm. Alongside is also displayed a fit to Eq. (1) and an experimental curve from extensive results on PS films [34]. This value of a_0 has been chosen to best match our DPLM results to the experimental results of PS films. $T_{g,\infty}$ is determined from the heat capacity of a bulk sample with periodic boundary conditions in all directions.

It is noteworthy that for the C_h curves during heating, thinner films begin to devitrify at much lower values of T in comparison to thicker films. For example, for $h = 10$, C_h has already increased significantly beyond 0 at $T \simeq 0.14$, well below $T_{g,h} \simeq 0.19$. This observation is consistent with the experimental findings reported in both bulk and film-polymer glasses [32,35–38].

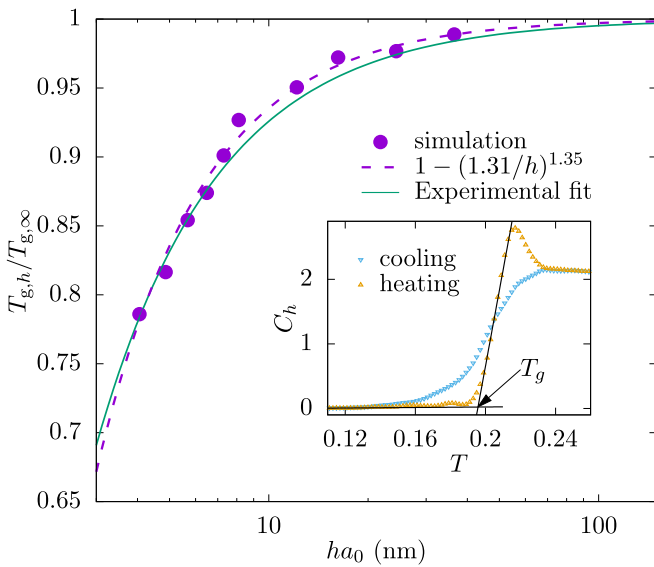


FIG. 3. Glass transition temperature $T_{g,h}$ against film thickness ha_0 with $a_0 = 0.81$ nm and $T_{g,\infty} = 0.198$. The experimental data for polystyrene films is taken from Ref. [34]. Inset: Heat capacity during cooling and heating for a film of thickness $h = 45$.

B. Glass transitions inferred from relaxation times

We employ the overlap function adopted in, e.g., Ref. [22] to study the structural relaxation of films. The overlap function gives the probability that a particle has no net movement after a time duration of t . We study both the overall overlap function for the whole film, defined by

$$q(t) = \langle \{1 - \Theta[|\mathbf{r}_i(t) - \mathbf{r}_i(0)|]\} \rangle, \quad (6)$$

and the depth-resolved overlap function, defined by

$$q_z(t) = \langle \{1 - \Theta[|\mathbf{r}_i(t) - \mathbf{r}_i(0)|]\} \rangle_z. \quad (7)$$

Here $\mathbf{r}_i(t)$ is the position of particle i at instant t . We average $q(t)$ over all particles and $q_z(t)$ over particles at depth z at time $t = 0$. The overall α -relaxation time $\tau_{\alpha,h}$ and depth-resolved α -relaxation time $\tau_{\alpha}(z)$ are defined by $q(\tau_{\alpha,h}) = q_z[\tau_{\alpha}(z)] = 1/e$, with e being the Euler constant. Figure 4 plots $\tau_{\alpha}(z)$ for a film with $h = 30$, demonstrating an acceleration of the structural relaxation near the free surface, similar to previous layer-resolved measurements [7,9]. We then obtain $T_g(z)$ as the temperature satisfying Deborah's condition [31],

$$\left. \frac{d\tau_{\alpha}(z)}{dT} \right|_{T=T_g(z)} = \frac{1}{Q_c}. \quad (8)$$

The local transition points $T_g(z)$ hence obtained are indicated in Fig. 4. Clearly, $T_g(z)$ depends on the cooling rate Q_c and our full results are displayed in Fig. 5, where it is seen that the layers near the free surface (i.e., $z < 5$) have substantially lower $T_g(z)$. For $z > 6$, $T_g(z)$ displays small spatial variation, showing that the substrate has little impact on the dynamics of the inner layers. We have extrapolated $\tau_{\alpha}(z)$ for layers with $T_g(z) < 0.18$, the lowest temperature that can be simulated.

In Fig. 6, we compare $T_{g,h}$ obtained from calorimetric measurements (solid circles) and from relaxation dynamics (triangles), and an agreement is achieved for the general trend. The purple triangles represent an arithmetic average of $T_g(z)$, i.e., $h^{-1} \int_0^h dz T_g(z)$. Such agreement implies a close relation

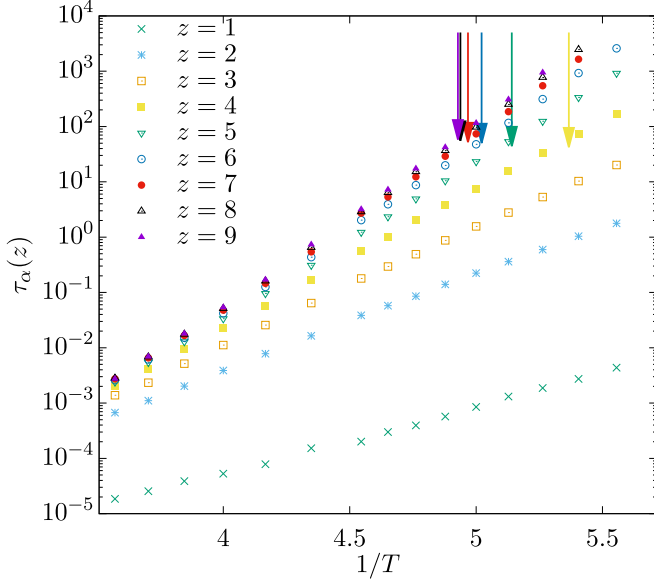


FIG. 4. The α -relaxation time of a $h = 30$ film at different depth z versus the inverse temperature $1/T$; the arrows indicate the location of local $T_g(z)$.

between the local structural relaxation and the calorimetric properties.

C. Layer contributions to film heat capacity

Finally, we show that the specific heat capacity $C_h(T)$ for a film can be reconstructed using its local relaxation time $\tau_\alpha(z)$. In the first place, we show that the specific heat capacity for a bulk sample is approximately a function of the reduced temperature $T/T_{g,\infty}$ for a narrow range of cooling rates; i.e., $C_\infty(T/T_{g,\infty})$ is roughly independent of cooling rate. This is demonstrated in Fig. 7. Further we propose that $C_h(T)$ can be approximated as an average over the layer heat capacity, approximated by $C_\infty[T/T_g(z)]$. This statement is described in

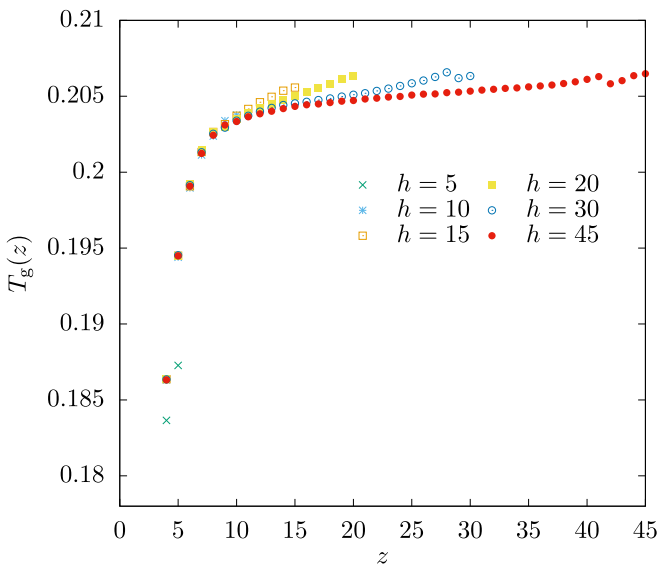


FIG. 5. $T_g(z)$ as determined using $\tau_\alpha(z)$ from Fig. 4.

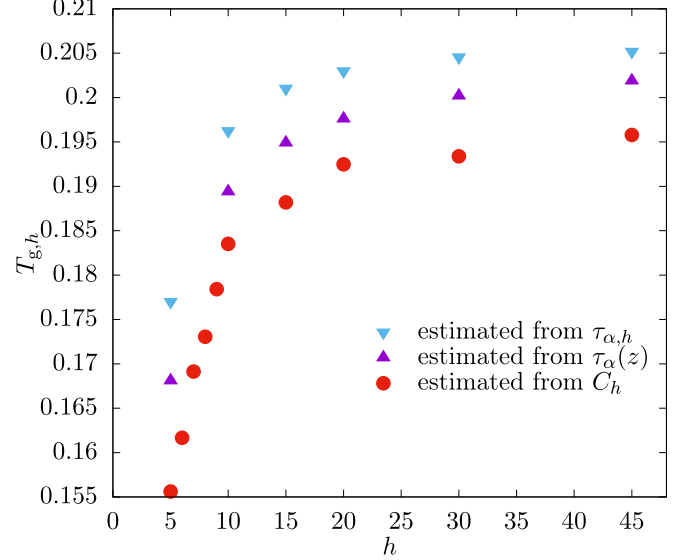


FIG. 6. Comparing $T_g(z)$ obtained from $\tau_{\alpha,h}$ (blue triangles), $\tau_\alpha(z)$ (purple triangles), and from the method shown in the inset of Fig. 3 (red circles) [30].

Eq. (2). The reconstructed heat capacity is shown as solid lines in Fig. 2. The results compare well with the direct calorimetric simulations (cf. symbols in Fig. 2). All the main features, including the overshoot along the heating path occurs at lower temperatures with smaller magnitude for thinner films.

Our reconstruction relies on the approximation that C_∞ only depends on the reduced temperature. This is accurate only for a narrow range of cooling rates. Yet the results are in reasonable agreement with directly simulated results.

IV. CONCLUSIONS

In conclusion, we have studied the interplay between the calorimetric properties and relaxation dynamics in DPLM films. The phenomenological Keddie-Cory-Jones relation between the glass transition temperature $T_{g,h}$ and film thickness for polystyrene thin films is well reproduced. We determine $T_{g,h}$ by the heat capacity curves as well as the α -relaxation time and the results agree nicely. This relates the nonequilibrium calorimetric properties of a film to their local structural relaxation time. Furthermore, we reconstructed the heat capacity of films with the aid of layer-resolved relaxation times.

Reproducing heat capacity curves of films by a lattice model affirms DPLM as a useful model for studying glassy systems. In this work, we have chosen model parameters appropriate for PS films. As a highly tunable model, the DPLM is expected to mimic the behaviors of a variety of glasses. The fragility can be controlled via parameters like G_0 [24]. The void density neighboring the free surface can be readily tuned by adjusting ϵ_{top} in Eq. (3), resulting in different strengths of surface enhancement. Similarly, a repulsive or attractive substrate can be modeled by tuning ϵ_{bot} . To date, thin-film phenomena such as a long-range (200–300 nm) gradient of glass transition temperature [19] or modulus [39], and surface enhanced dynamics penetrating into the films as deep as

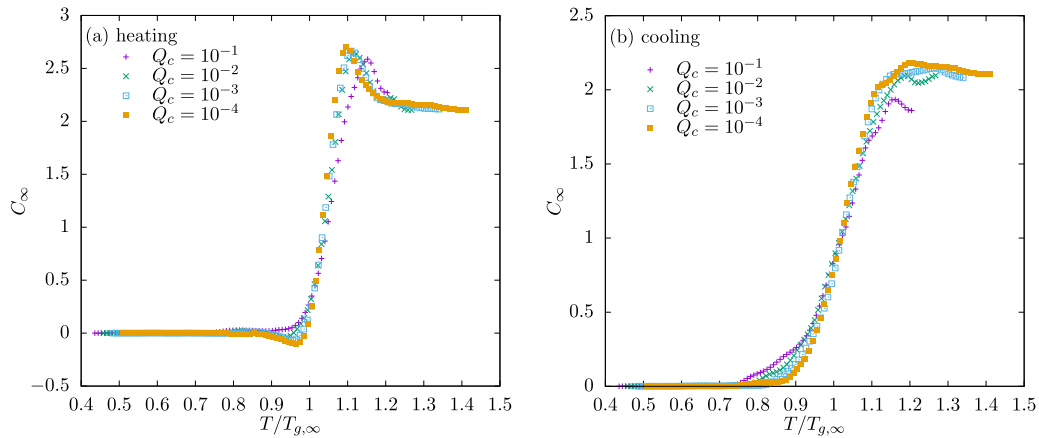


FIG. 7. Specific heat capacity C_∞ versus the reduced temperature $T/T_{g,\infty}$ at various cooling rates Q_c . (a) Heating process; (b) cooling process.

micrometers [40] have not been fully understood; they can be studied by our model in the future.

ACKNOWLEDGMENTS

This work was supported by China Postdoc Fund Grant No. 2022M722548, Shaanxi NSF Grant No.

2023-JC-QN-0018, Central University Basis Research Fund Grant No. xzy012023044, National Natural Science Foundation of China Grant No. 12405042, Hong Kong GRF Grant No. 15303220, and National Key Research and Development Programs No. 2020YFB2007901 and No. 2022YFE0109500.

-
- [1] K. Binder and W. Kob, *Glassy Materials and Disordered Solids: An Introduction to Their Statistical Mechanics* (World Scientific, Singapore, 2011).
- [2] G. Biroli and J. P. Garrahan, Perspective: The glass transition, *J. Chem. Phys.* **138**, 12A301 (2013).
- [3] G. B. McKenna and S. L. Simon, 50th anniversary perspective: Challenges in the dynamics and kinetics of glass-forming polymers, *Macromolecules* **50**, 6333 (2017).
- [4] S. Napolitano, E. Glynos, and N. B. Tito, Glass transition of polymers in bulk, confined geometries, and near interfaces, *Rep. Prog. Phys.* **80**, 036602 (2017).
- [5] F. Arceri, F. P. Landes, L. Berthier, and G. Biroli, Glasses and aging, a statistical mechanics perspective on, in *Statistical and Nonlinear Physics* (Springer, Berlin, 2022), p. 229.
- [6] J. L. Keddie, R. A. L. Jones, and R. A. Cory, Size-dependent depression of the glass transition temperature in polymer films, *Europhys. Lett.* **27**, 59 (1994).
- [7] F. Varnik, J. Baschnagel, and K. Binder, Reduction of the glass transition temperature in polymer films: A molecular-dynamics study, *Phys. Rev. E* **65**, 021507 (2002).
- [8] J. S. Sharp and J. A. Forrest, Free surfaces cause reductions in the glass transition temperature of thin polystyrene films, *Phys. Rev. Lett.* **91**, 235701 (2003).
- [9] J. Baschnagel and F. Varnik, Computer simulations of supercooled polymer melts in the bulk and in confined geometry, *J. Phys.: Condens. Matter* **17**, R851 (2005).
- [10] S. Kim, S. A. Hewlett, C. B. Roth, and J. M. Torkelson, Confinement effects on glass transition temperature, transition breadth, and expansivity: Comparison of ellipsometry and fluorescence measurements on polystyrene films, *Eur. Phys. J. E* **30**, 83 (2009).
- [11] Z. Yang, Y. Fujii, F. K. Lee, C.-H. Lam, and O. K. C. Tsui, Glass transition dynamics and surface layer mobility in unentangled polystyrene films, *Science* **328**, 1676 (2010).
- [12] C.-H. Lam and O. K. C. Tsui, Crossover to surface flow in supercooled unentangled polymer films, *Phys. Rev. E* **88**, 042604 (2013).
- [13] R. R. Baglay and C. B. Roth, Local glass transition temperature $T_g(z)$ of polystyrene next to different polymers: Hard vs. soft confinement, *J. Chem. Phys.* **146**, 203307 (2017).
- [14] C.-H. Lam, Deeper penetration of surface effects on particle mobility than on hopping rate in glassy polymer films, *J. Chem. Phys.* **149**, 164909 (2018).
- [15] K. S. Schweizer and D. S. Simmons, Progress towards a phenomenological picture and theoretical understanding of glassy dynamics and vitrification near interfaces and under nanoconfinement, *J. Chem. Phys.* **151**, 240901 (2019).
- [16] C. B. Roth, Polymers under nanoconfinement: Where are we now in understanding local property changes? *Chem. Soc. Rev.* **50**, 8050 (2021).
- [17] A. Ghanekarade, A. D. Phan, K. S. Schweizer, and D. S. Simmons, Signature of collective elastic glass physics in surface-induced long-range tails in dynamical gradients, *Nat. Phys.* **19**, 800 (2023).
- [18] R. D. Priestley, D. Cangialosi, and S. Napolitano, On the equivalence between the thermodynamic and dynamic measurements of the glass transition in confined polymers, *J. Non-Cryst. Solids* **407**, 288 (2015).
- [19] R. R. Baglay and C. B. Roth, Experimental study of the influence of periodic boundary conditions: Effects of finite size and faster cooling rates on dissimilar polymer-polymer interfaces, *ACS Macro Lett.* **6**, 887 (2017).

- [20] J. H. Mangalana, M. E. Mackura, M. D. Marvin, and D. S. Simmons, The relationship between dynamic and pseudo-thermodynamic measures of the glass transition temperature in nanostructured materials, *J. Chem. Phys.* **146**, 203316 (2017).
- [21] S. Peter, H. Meyer, J. Baschnagel, and R. Seemann, Slow dynamics and glass transition in simulated free-standing polymer films: a possible relation between global and local glass transition temperatures, *J. Phys.: Condens. Matter* **19**, 205119 (2007).
- [22] M. Lulli, C.-S. Lee, H.-Y. Deng, C.-T. Yip, and C.-H. Lam, Spatial heterogeneities in structural temperature cause kovacs' expansion gap paradox in aging of glasses, *Phys. Rev. Lett.* **124**, 095501 (2020).
- [23] M. Lulli, C.-S. Lee, L.-H. Zhang, H.-Y. Deng, and C.-H. Lam, Kovacs effect in glass with material memory revealed in non-equilibrium particle interactions, *J. Stat. Mech.* (2021) 093303.
- [24] C.-S. Lee, M. Lulli, L.-H. Zhang, H.-Y. Deng, and C.-H. Lam, Fragile glasses associated with a dramatic drop of entropy under supercooling, *Phys. Rev. Lett.* **125**, 265703 (2020).
- [25] C.-S. Lee, H.-Y. Deng, C.-T. Yip, and C.-H. Lam, Large heat-capacity jump in cooling-heating of fragile glass from kinetic Monte Carlo simulations based on a two-state picture, *Phys. Rev. E* **104**, 024131 (2021).
- [26] X.-Y. Gao, H.-Y. Deng, C.-S. Lee, J. You, and C.-H. Lam, Emergence of two-level systems in glass formers: A kinetic Monte Carlo study, *Soft Matter* **18**, 2211 (2022).
- [27] G. Gopinath, C.-S. Lee, X.-Y. Gao, X.-D. An, C.-H. Chan, C.-T. Yip, H.-Y. Deng, and C.-H. Lam, Diffusion-coefficient power laws and defect-driven glassy dynamics in swap acceleration, *Phys. Rev. Lett.* **129**, 168002 (2022).
- [28] X.-Y. Gao, C.-Y. Ong, C.-S. Lee, C.-T. Yip, H.-Y. Deng, and C.-H. Lam, Kauzmann paradox: A possible crossover due to diminishing local excitations, *Phys. Rev. B* **107**, 174206 (2023).
- [29] Q. Zhai, X.-Y. Gao, C.-S. Lee, C.-Y. Ong, K. Yan, H.-Y. Deng, S. Yang, and C.-H. Lam, Surface mobility gradient and emergent facilitation in glassy films, *Soft Matter* **20**, 4389 (2024).
- [30] Y.-Z. Yue, Characteristic temperatures of enthalpy relaxation in glass, *J. Non-Cryst. Solids* **354**, 1112 (2008).
- [31] I. Hodge, Enthalpy relaxation and recovery in amorphous materials, *J. Non-Cryst. Solids* **169**, 211 (1994).
- [32] N. G. Perez-de Eulate, V. Di Lisio, and D. Cangialosi, Glass transition and molecular dynamics in polystyrene nanospheres by fast scanning calorimetry, *ACS Macro Lett.* **6**, 859 (2017).
- [33] C. Rodríguez-Tinoco, M. Gonzalez-Silveira, J. Ràfols-Ribé, A. Vila-Costa, J. C. Martinez-Garcia, and J. Rodríguez-Viejo, Surface-bulk interplay in vapor-deposited glasses: Crossover length and the origin of front transformation, *Phys. Rev. Lett.* **123**, 155501 (2019).
- [34] J. A. Forrest and K. Dalnoki-Veress, The glass transition in thin polymer films, *Adv. Colloid Interface Sci.* **94**, 167 (2001).
- [35] D. Cangialosi, V. M. Boucher, A. Alegría, and J. Colmenero, Direct evidence of two equilibration mechanisms in glassy polymers, *Phys. Rev. Lett.* **111**, 095701 (2013).
- [36] N. G. Perez-De Eulate and D. Cangialosi, The very long-term physical aging of glassy polymers, *Phys. Chem. Chem. Phys.* **20**, 12356 (2018).
- [37] X. Monnier and D. Cangialosi, Thermodynamic ultrastability of a polymer glass confined at the micrometer length scale, *Phys. Rev. Lett.* **121**, 137801 (2018).
- [38] Z. Song, C. Rodríguez-Tinoco, A. Mathew, and S. Napolitano, Fast equilibration mechanisms in disordered materials mediated by slow liquid dynamics, *Sci. Adv.* **8**, eabm7154 (2022).
- [39] Y. J. Gagnon, J. C. Burton, and C. B. Roth, Development of broad modulus profile upon polymer–polymer interface formation between immiscible glassy–rubbery domains, *Proc. Natl. Acad. Sci. USA* **121**, e2312533120 (2024).
- [40] H. Yuan, J. Yan, P. Gao, S. K. Kumar, and O. K. Tsui, Microscale mobile surface double layer in a glassy polymer, *Sci. Adv.* **8**, eabq5295 (2022).